Webology, Volume 18, Number 5, 2021
ISSN: 1735-188X
DOI: 10.29121/WEB/V18I5/42

VHF Bands Compact Transmitter Manufacturing and Design Utilizing Composite Right/Left-handed Fibreoptic Cables

Ashutosh Dixit[1], Sandeep Sunori[2], Parvesh Saini[3]

[1]Department of Electrical Engineering,Graphic Era Deemed to be University, Dehradun, Uttarakhand India, 248002
[2]Department of Electronics & Communication Engineering, Graphic Era Hill University, Bhimtal, Uttarakhand India, 263156
[3]Department of Electrical Engineering,Graphic Era Deemed to be University, Dehradun, Uttarakhand India, 248002

ABSTRACT

A certain study describes a tiny short-wave antenna that employs a hybrid absolutely correct power line. These suggested antennae contain interdental capacitance as well as shunted helical inductive loads in 4- as well as 6-unit blocks. At 170 MHz, the satellite's diameter of 4-unit columns is 0.0410µ, 0450µ, 0048µ, as well as its highest efficiency is 35 percent on average. The antenna is made with production order cells to improve the efficiency. It has a width of 0.0410µ, 0450µ, 0048µ over 171.25 Ghz with a generating power of 39 dBi. All transmitters have an infrared spectrum. Every antenna has an electromagnetic capacity in kV of 0.0365 et 0.25, correspondingly. These impacts of distributed element bandwidth on transmission lines were examined. The impact of the distributed element input signal on input impedance was also explored. The Reconnect TL-based antenna may transcend the radio mechanical limitations of traditional defined antennas. As little more than a result, the suggested antennas are suitable for radio communications in the frequency range.

Keywords: VHF band; Transmitter; Design; CRLH; Fibreoptic Caple; Radiation Pattern.

INTRODUCTION

Metamaterial antennae, diagonal transmitters, as well as whip satellite dishes are commonly used in communications equipment inside the band. Because the size of those antennas was related to bandwidth, devices have significant manoeuvrability and efficiency disadvantages within the MHz range. Smaller stations inside the Vhf and uhf were developed to address such drawbacks. Nanoscale transmitters come in a variety of shapes and sizes. Compact antennae with blended proper overhead lines have suddenly received a lot of attention [1]. Quarter wavelength TL exhibits LH properties at low frequencies and blood group properties at frequencies. The transmission constants change from negative to positive as the current increases from minimum to maximum, and

Webology, Volume 18, Number 5, 2021
ISSN: 1735-188X
DOI: 10.29121/WEB/V18I5/42

the parallel-coupled Lc architecture must have the smallest inductance, which can be reduced by using a capacitor.

It's still difficult to avoid stress on the body intractably in circuits, which is like dislocation as well as stretched tension, rendering this more susceptible than rigid alternatives. Liquid commodity prices have distinguishable self-importance skills as laminates, including flowing fluid aided connections, stretchable signal conditioning, and thermoelectric initiation, and thus eventually wind up influencing this same elastomeric conceptual model individuality as well as the independent digital identification of powder material droplets ingrained in silicone dynamic recrystallization [2,3]. However, current difficulties like motivation, DC power supply gear, lengthy servicing intervals, networking stability, and capability restoration after repair lifetime are still more complex.

As little more than a result, discovering a technology which can recover not only the structure but also electrical operation in a simple, quick, or maybe even item of information way employing a 3-dimensional applaudingly magnetic device has become more important in flexible sensors. Due to their decreased viscosity, flowing metals are deemed inappropriate for a broad range of materials. However, an oxidising reactionist at a height of about 3 nm inside the gaseous phase might occur due to the presence. Aluminium is suggested to assist students to make connections to encourage combo formation with different metal particles, resulting in the see beck coefficient, tension durability, and almost adhesive capacities of polymer composites [4].

As nothing more than a result, we demonstrate throughout this study that magnetically attached flow substance elasticity systems could have good remote spirit, fluid, and thermal transference imprinted characteristics, permitting several functionalities on a given solid support. These gadgets are comprised of three major components: liquid anodized metal (Fe-GaIn), a disposable PVD layer, and stickiness glucose. Some of these could result in yet another performance. A flexible magma amalgam will just be precisely pressed further along the motion of the magnets to repair whatever conduction places are vacant whenever real damage happens inside a short perioperative period through employing the weird environment of nanocrystals underneath a magnetic field. Its PVP base must absorb, and the conductive elastic threads that hold magnetic liquid elements must be easily recoverable and reusable [5].

Smaller antennae based on parallel-coupled Tr were extensively researched inside the frequency range. Nevertheless, research on VHF towers employing parallel-coupled TL appears to be sparse. An antenna constructed on parallel-coupled Tp is created for the frequency range of research. The suggested antennas feature three-or seven-unit cells made up of interdental capacitance and shunted helical inductances. This directional antenna length using four crystal structures is 0.041 0.045 0.048 for 171 GHz, with an average efficiency of 35%. This antenna is made of 6-unit cells that boost the efficiency. It has a size of 0.041 0.045 0.048 at 171.5MHz with a peak gain of 33.62 dBi. Every antenna has an electromagnetic capacity in kR of 0.045 to 0.25 [6,7].

The letter 'k' represents the resonant frequency. The diameter of the largest hemispheric which can contain the antennas is indeed the actual dimension 'r.' Extremely tiny antennae are transmitters and receivers with diameters less than 0.3 kl. As a result, the suggested antennae were extremely tiny.

Webology, Volume 18, Number 5, 2021
ISSN: 1735-188X
DOI: 10.29121/WEB/V18I5/42

These implications of series connected amplitude on a wide band are, however, examined.

DESIGN OF CLRH

Figure 1 depicts a reconnect power station step response. Because a moved (LH) waveguide comprises of either a step-down transformer as well as a shunted circuit, an electromagnetic mixture of fuel exists between converters, resulting in parasitic functionality inside the transmitter. The top conductor and the side of the substrate both create parasitic equivalent capacitors. As a result of such occurrences, an Rh transient stability development dimension RH characteristic is formed. Parallel-coupled TL seems to have the lowest inductance when the transmission coefficient () approaches negative, allowing smaller antennae to be used. In the instance of open termination, the drain input impedance determines its integrand vibration.

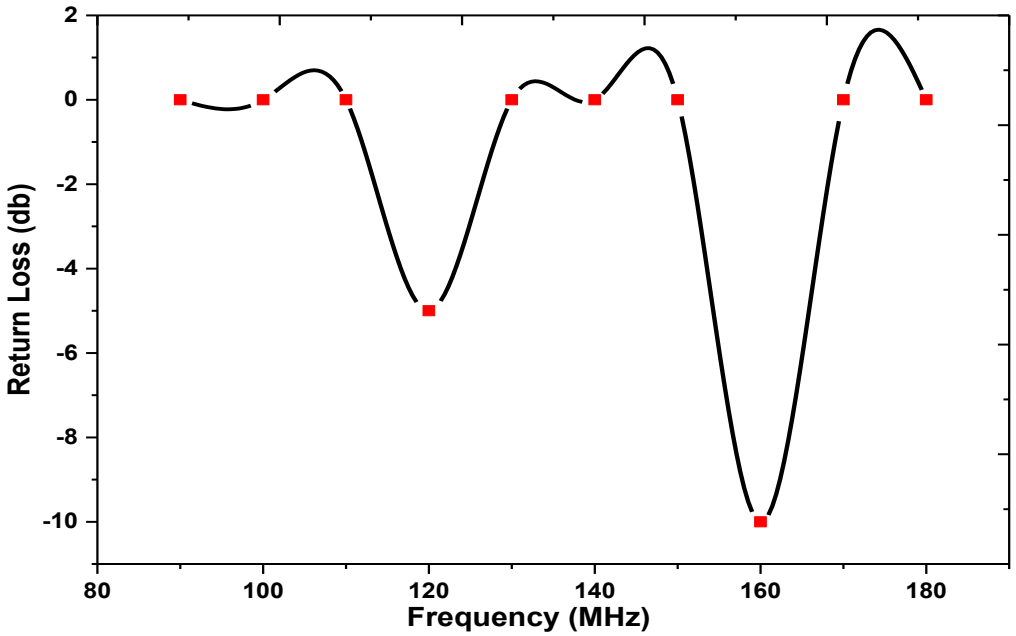

Fig.1. Return loss of CLLR based on the frequency

This is made up of a parallel helical inductance as well as a lateral capacitance. The equivalent impedance of the interdental resistor (CL) Its shunted capacitance (LL) is constructed from a helical capacitor and just a through as previously stated, the drain capacitor (CR) as well as the serial inductor (LR) constitute parasite variables. The integrand resonant of a crystal lattice is optimised at 170 MHz using the Simulink Flow simulation programme [8]. Its substrates are Taconic TLY with a depth of 1.52 cm, while the following table displays the optimum tetragonal parameters. Its cells are 0.0110µ, 0350µ, 048µ in size. The helical inductance (LL) seems to have a permeability of 98.4 nm as well as a discharge capacitor of 9.84 pF. A through-connects the helical inductance towards the antenna array. Its construction is seen in Figure 1. Simulink Flow simulation designed the antennae. It has four-unit cells with a size of 0.0410µ, 0450µ, 048µ at 171 MHz. The satellite's electromagnetic dimension, mm kr, was 0.362. Figure 2 depicts this directional antenna reflection

Webology, Volume 18, Number 5, 2021
ISSN: 1735-188X
DOI: 10.29121/WEB/V18I5/42

coefficient degradation pattern. 171 MHz is indeed the smallest absorption coefficient.

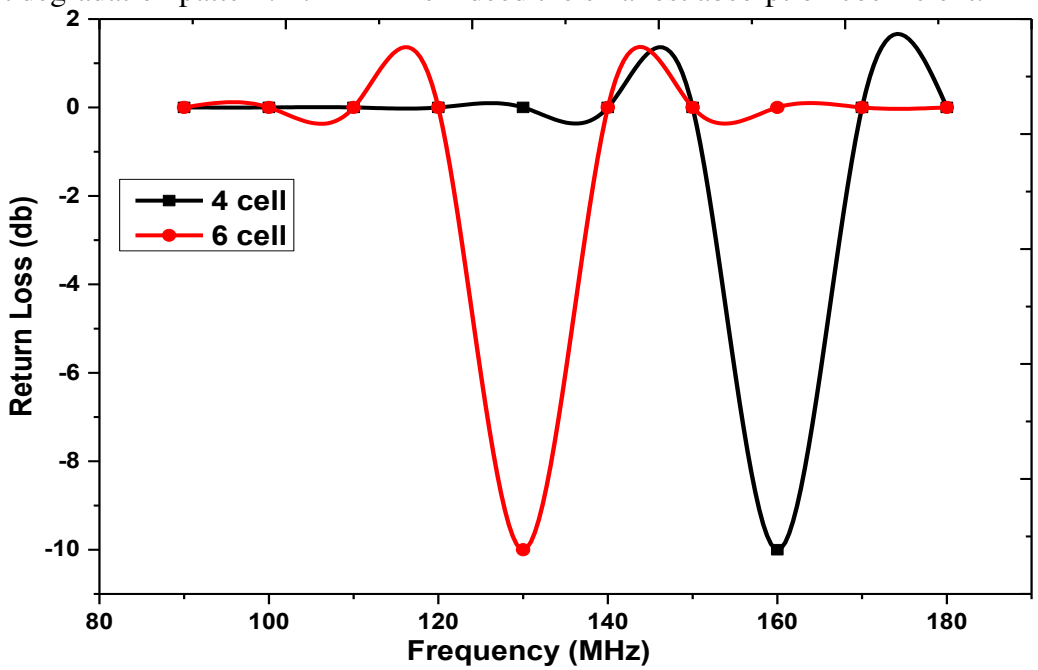

Fig.2. Return loss of CLLR 3 cell antenna and 6 cell mis matched antenna based on the frequency

The directional antenna bitrate at integrand resonance is 0.20%. 1 game's phase shift is 149 MHz. Figure 3 demonstrates typical electromagnetic felder concentrations at integrand resonance using four components at 171 MHz. Owing to the negative phasing characteristic (=0), there isn't any phase shift of a field. Figure 3 depicts the numerical model of a satellite's normalised output waveform. This antenna emits bidirectional irradiation with a maximum efficiency of 43 dBi. They designed an antenna using additional parallel-coupled TL unit cells that produce radio efficiency. Figure 3 depicts a parallel-coupled TL antenna having six hexagonal lattices. It has a true size of 0.0410μ, 0450μ, 048μ as well as an electric length of 0.25 [9].

Even though yield for tiny antennae is related to narrow bandwidth, expanding the amount of hexagonal lattice can improve the signal to noise ratio. Nevertheless, when the number of monolayers rises, an inductance imbalance emerges. Both the intake reactance of a thing made of cell antennas and the voltage unmatched 7 cell antennas are shown in Figure1. It is worth noting that perhaps the cell proliferates antennas have their harmonic oscillator resonant at 171 MHz, whereas the 7 cell antennas don't seem to. Two inductance enabling M o reflection coefficient are included in the suggested six cellular antennas. Figure 2 displays the estimated impedance also during performing our N's match. 173 Ghz is indeed the zeroth electric potential.

The harmonic oscillator radiation pattern is nearly identical to a multiple antenna resonance. Figure 2 depicts the normalised reflection coefficient simulation model. This antenna is horizontal and has a maximum efficiency of 36.25 dBi. When compared to four crystal structures, the intensity is increased by 7 dBi [10].

Webology, Volume 18, Number 5, 2021
ISSN: 1735-188X
DOI: 10.29121/WEB/V18I5/42

FABRICATION AND MEASUREMENT

Figure 3 depicts the antennae that were created. For transmission lines, the L-section equivalent circuit by a Ct Activities CI-BI0231 parallel chip capacitor with a frequency of 280 nH as well as a Ct Catechu CI-B17125-191 shunted inductance only with a frequency of 180 nH is employed. Fig. 11 depicts the expected and observed impedance of a various cell antennas. The correlation across manual calculations is excellent. At 171 MHz, its input impedance is 11.36 decibels. Figure 3 depicts both the calculated impedance of an antenna having a 7-hexagonal lattice and the calculations. Both integrand frequency responses were nearly identical at 172.4 MHz, but the correlation coefficients increased differently than each modelling estimate. This manufactured antenna has a frequency spectrum of 3.96%, whereas the modelled dipole has a lower frequency of 0.29%. To investigate the inaccuracy, the antennas' component aggregated inductances were assessed to achieve optimum internal resistance [11].

Both reported as well as predicted intake impedances of 6 column antennae are shown in Figure 3. It is possible to demonstrate that the observed input resistance has a lower average than each modelled insertion loss and, therefore, that their imagined portions are nearly equal. Figures 1 and 2 display the current currents and voltages obtained via shunt and serial inductance tests, respectively. Again, using a numerical method, researchers evaluated the radiation pattern without any parallel combination. Its omnidirectional antenna susceptibility was again determined using the aggregated part. You may isolate the real resistivity of the inductances as well as derive their frequency characteristics by simply reducing overall impedances without any inductors and capacitors from that after the inductances.

Figure 3 depicts both received and computed information. This computed information is gathered by measuring the satellite's insertion loss without capacitances and then extracting the inductance thereof. Because real capacitances were employed inside the study, the comparison between the computed and observed tables reveals considerable overlap. Researchers discovered that now the lumpy item's real susceptibility differs through its idealised admittance. It indicates that even if you utilise all optimal ratios of aggregated parts in capacitance balancing, you will have a switching loss. As a result, both the periodic signal characteristics of aggregated parts as well as the directional antennas' real resistance.

Webology, Volume 18, Number 5, 2021
ISSN: 1735-188X
DOI: 10.29121/WEB/V18I5/42

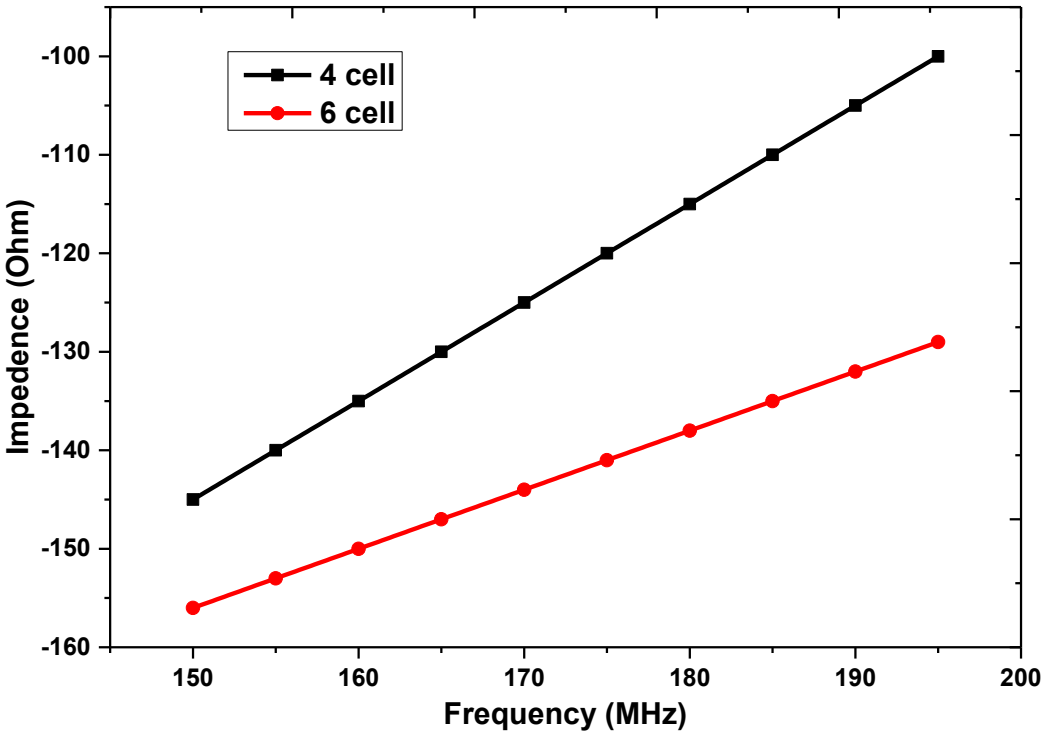

Fig.3. Input impedance of two different cells

CONCLUSION

Somewhere in the Uwe band, compact antennae made of quarter wavelength TL were developed and built. These suggested antennae are made up of 3-as well as 6-unit cells made up of interdental capacitance as well as shunted helical inductances. At 171 MHz, a dipole using three monolayers does indeed have a size of 0.0410.4550.048 as well as a maximum efficiency of 36 dBi. The length of 6 cell antennas at 161.4 MHz is 0.041 0.045 0.048, and the maximum gain is 26.5 dBi. Its beamwidth is again given by the number of hexagonal lattices. The impact of monolithic integrated circuits on transmission lines has been further explored. A contributing, meaningfully TL-based radiator may transcend the radio structural limitations of traditional combat antennas. As a result, these suggested antennae could be employed for defence equipment.

REFERENCES

1. Choi, J.; Cheon, H.; Choi, J.; Kim, H.; Cho, J.; Kim, S.; Studies, A. A Study on Insulation Characteristics of Laminated Polypropylene Paper for an HTS Cable. 2010, 20, 1280–1283.
2. Awang, M.; Ismail, H.Ã.; Hazizan, M.A. ARTICLE IN PRESS POLYMER Processing and Properties of Polypropylene-Latex Modified Waste Tyre Dust Blends (PP / WTD ML). 2008, 27, 93–99, doi:10.1016/j.polymertesting.2007.09.008.
3. Yuan, Z.; Tu, Y.; Li, R.; Zhang, F.; Gong, B.; Wang, C. Review on the Characteristics , Heating Sources and Evolutionary Processes of the Operating Composite Insulators with Abnormal Temperature Rise. 2022, 8, 910–921, doi:10.17775/CSEEJPES.2019.02790.
4. Kap, J.; Kyu, J.; Kim, T.; Sang, K.; Ki, R.; Chung, S. Method for Determining Dissipation Factor of Capacitors Without Reference Capacitor at Voltages up to 1 KV. J. Electr. Eng.

Webology, Volume 18, Number 5, 2021
ISSN: 1735-188X
DOI: 10.29121/WEB/V18I5/42

Technol. 2019, 14, 371–376, doi:10.1007/s42835-018-00007-7.

5. Kitoh, Y.; Noguchi, Y.; Design, A.H.T.S.C. Test Results of a 30 m HTS Cable for Yokohama Project. 2011, 21, 1030–1033.
6. Bantien, F.; Marek, J.; Willmann, M. Silicon Pressure Sensor with Integrated CMOS Sign & Conditioning Circuit and Compensation of Temperature Coefficient. 1991, 27, 21–26.
7. Jousset, P.; Reinsch, T.; Ryberg, T.; Blanck, H.; Clarke, A.; Aghayev, R.; Hersir, G.P.; Henninges, J.; Weber, M.; Krawczyk, C.M. Structural Features. 2018, doi:10.1038/s41467-018-04860-y.
8. Kuvshinov, B.N. Interaction of Helically Wound Fibre-Optic Cables with Plane Seismic Waves. 2016, 671–688, doi:10.1111/1365-2478.12303.
9. Bakker, M.; Calj, R. An Active Heat Tracer Experiment to Determine Groundwater Velocities Using Fiber Optic Cables Installed with Direct Push Equipment.
10. Mamer, E.A.; Lowry, C.S. Locating and Quantifying Spatially Distributed Groundwater / Surface Water Interactions Using Temperature Signals with Paired Fiber-Optic Cables. 2013, 49, 7670–7680, doi:10.1002/2013WR014235.
11. Msongaleli, D.L.; Dikbiyik, F.; Zukerman, M.; Mukherjee, B. Disaster-Aware Submarine Fiber-Optic Cable Deployment for Mesh Networks. 2016, 8724, 1–11, doi:10.1109/JLT.2016.2587719.